

Taking snapshots of a quantum thermalization process: emergent classicality in quantum jump trajectories

Charlie Nation*

Department of Physics and Astronomy, University of Sussex, Brighton, BN1 9QH, United Kingdom.

Diego Porras†

Institute of Fundamental Physics, IFF-CSIC, Calle Serrano 113b, 28006 Madrid, Spain

(Dated: May 29, 2022)

We theoretically investigate the emergence of classical statistical physics in a finite quantum system that is subjected to a quantum measurement process. A random matrix theory approach to non-integrable quantum systems predicts that the set of outcomes of the measurement of a macroscopic observable evolve in time like stochastic variables, whose variance satisfies the celebrated Einstein relation for Brownian diffusion. Our results show how to extend the framework of eigenstate thermalization to the prediction of properties of quantum measurements on an otherwise closed quantum system. We show numerically the validity of the random matrix approach in quantum chain models.

Introduction:– Quantum non-equilibrium dynamics raises intriguing questions only recently addressed in experiments [1–6]. These include how and under what conditions isolated many-body quantum systems equilibrate to a thermal state [7–14] – a process known as quantum thermalization [15–19]. Important open questions remain surrounding relaxation time-scales and the route to equilibrium of complex quantum systems [20–28], as well as the emergence of thermodynamical laws [29–32]. A useful approach to the description of generic non-integrable quantum systems can be developed from quantum chaos [33, 34] and the eigenstate thermalization hypothesis (ETH), which in turn can be derived from an underlying random matrix theory (RMT) [24, 35], based on Deutsch’s model [25, 36–38] for non-integrable systems.

Most works on quantum thermalization dynamics focus on the evolution of expectation values of local operators, $\langle O(t) \rangle$. In a typical experiment, however, a set of quantum measurements at times t_1, t_2, \dots , generates a set of outcomes O_1, O_2, \dots . Here, a few natural questions arise: Do the observation outcomes have the properties of a classical stochastic trajectory in the appropriate limit? How do thermodynamical properties of stochastic trajectories emerge within the RMT and ETH picture? How different are the dynamics of expectation values, $\langle O(t) \rangle$, compared to the set of measurements obtained under continuous monitoring? Answering those questions is not only of fundamental interest, but can also lead to novel ways of characterizing quantum devices.

We address the questions above within the theoretical framework of RMT and quantum chaotic wavefunctions [35] applied to a quantum quench scenario. Firstly, we take the more conventional point of view in which the system evolves up to a certain time, t , at which a quantum measurement of a local operator is performed. We focus on the variance of measured values of O after a series of experimental runs, σ_O^2 , and we show that, at

long times, it satisfies the celebrated Einstein relation, $\sigma_O^2 \propto k_B T$, with T the microcanonical temperature, provided certain conditions are met by O . Then we move on to the case in which the system is continuously monitored during the thermalization process [39], yielding a set of measurement outcomes, O_j , at times $t_j = j\Delta t$.

Within the RMT approach to non-integrable systems, we show that the measured values O_j are a set of stochastic variables that follow a Markov process with a typical relaxation rate Γ . Our model describes emergence of Brownian motion dynamics *in a closed quantum system subjected to a quantum measurement*. We also show that there exists a quantum Zeno regime for very short Δt , in which equilibration slows down. Finally, our approach can be exploited to measure the density of states (DOS) of the system as the ratio between time-integrated fluctuations of $\langle O(t) \rangle$ and the variance of quantum measurement outcomes. We numerically check our results in quantum chain models.

Set up:– Consider an isolated finite quantum system separated into a ‘(sub)system’ S , and ‘bath’ B . The system Hilbert space is defined as the support of a local observable of interest. The interacting Hamiltonian is $H = H_0 + V$, with $H_0 = H_S \otimes \mathbb{1}_B + \mathbb{1}_S \otimes H_B$, where $\mathbb{1}_{S(B)}$ is the identity on the system (bath) Hilbert space. Note that the system Hilbert space can correspond to local degrees of freedom in an homogeneous system, or a system weakly coupled to a finite bath.

We define the basis of eigenstates of H_S and H_B ,

$$\begin{aligned} H_S |\epsilon_s\rangle &= \epsilon_s |\epsilon_s\rangle, \quad s = 1, \dots, d_S, \\ H_B |E_\beta^{(B)}\rangle &= E_\beta^{(B)} |E_\beta^{(B)}\rangle, \quad \beta = 1, \dots, d_B. \end{aligned} \quad (1)$$

The (free) eigenstates of H_0 are $|\phi_\alpha\rangle$, with energy E_α , and we define the index $\alpha = 1, \dots, d_S d_B$, in order of increasing energy ($E_{\alpha+1} > E_\alpha$). Free eigenstates can be written as $|\phi_\alpha\rangle = |\epsilon_s\rangle |E_{\beta=f(\alpha,s)}^{(B)}\rangle$, with $f(\alpha, s)$ defined by the energy matching, $E_{f(\alpha,s)}^{(B)} = E_\alpha - \epsilon_s$. The (interacting)

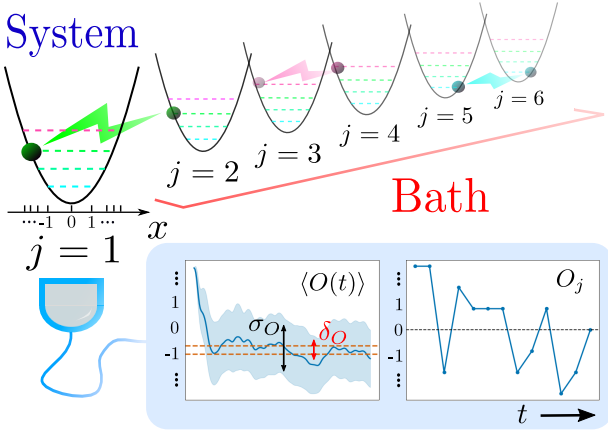


FIG. 1. Diagram of general scheme. We consider systems with many energy levels, and thus many possible observable outcomes (diagram of Hamiltonian (15)). Local system observables may be measured via expectation value $\langle O(t) \rangle$ or via sequence of projective measurements O_j .

eigenstates of the total Hamiltonian H are written as $|\psi_\mu\rangle = \sum_\alpha c_\mu(\alpha)|\phi_\alpha\rangle$. The total and bath DOS at energy E are $D(E)$ and $D_B(E)$, respectively. In the limit of large system sizes they are related via:

$$D(E_\alpha) = \sum_s D_B(E_\alpha - \epsilon_s), \quad (2)$$

which essentially counts the number of states of the bath that match the energies of the system.

Consider a local observable $O = O_S \otimes \mathbb{1}_B$. We define operator matrix elements in the interacting basis by subscripts μ, ν , $O_{\mu\nu} := \langle \psi_\mu | O | \psi_\nu \rangle$, and free basis by subscripts α, β , $O_{\alpha\beta} := \langle \phi_\alpha | O | \phi_\beta \rangle$. Non-interacting matrix elements can, in turn, be written in terms of local and bath degrees of freedom like $\langle \phi_\alpha | O | \phi_\beta \rangle = (O_S)_{s(\alpha)s(\beta)} \delta_{\alpha_B(\alpha)\alpha_B(\beta)}$, where $s(\alpha)$ and $\alpha_B(\alpha)$ are the system and bath quantum numbers, respectively, of the free eigenstate α .

Random Matrix Approach:— Studying the local dynamics of a generic many-body systems is a challenging task. Our approach here involves a drastic simplification, namely, we assume that V is a real symmetric random matrix. This assumption directly leads to the ETH, and also to effects that have been thoroughly checked in numerics in a variety of non-integrable systems [35, 41? – 43]. Formally, we express the matrix elements of V in the free basis as random Gaussian numbers with $\langle V_{\alpha\beta} \rangle_V = 0$ and $\langle V_{\alpha\beta}^2 \rangle_V = \frac{g^2(1+\delta_{\alpha\beta})}{N}$, where $\langle \dots \rangle_V$ indicates an ensemble average over realizations of V . Furthermore, we assume that $(H_0)_{\alpha\beta} = \alpha\omega_0\delta_{\alpha\beta}$, with $\omega_0 = 1/N$. This last approximation only involves neglecting the variations in DOS within a relevant energy width (to be properly defined below).

The eigenstates of H can be shown to follow a

Lorentzian distribution [36, 44],

$$\langle c_\mu^2(\alpha) \rangle_V := \Lambda(\mu, \alpha) = \frac{\omega_0 \Gamma / \pi}{(E_\mu - E_\alpha)^2 + \Gamma^2}, \quad (3)$$

with $\Gamma = \frac{\pi g^2}{N\omega_0}$ [35].

In Ref. [35] the current authors showed that this model leads to observable matrix elements, $O_{\mu\nu}$, in agreement with the ETH ansatz [34, 45]. This is achieved using a statistical theory of eigenstate correlation functions $\langle c_\mu(\alpha)c_\nu(\beta)\dots \rangle_V$. Our model of chaotic wavefunctions can be shown to be self-averaging [46], and thus taking the ensemble average to obtain such correlation functions is justified. See supplemental material (SM) [47] for technical details.

Continuing, we assume that the initial state for the quantum quench is an eigenstate of H_0 , $|\psi(0)\rangle = |\phi_{\alpha_0}\rangle$, with eigenenergy E_{α_0} , though the formalism is easily extended to more general cases [24]. We focus local observables that are diagonal in the free basis, $O_{\alpha\beta} \propto \delta_{\alpha\beta}$. Our RMT model assumes a constant DOS, $1/\omega_0$, and coupling, g , leading also to a quantum chaotic eigenfunction width, Γ , that is independent of the energy. This theory can be applied to a generic quantum many-body system by the substitution $1/\omega_0 \rightarrow D(E_{\alpha_0})$. The RMT predictions are valid as long as variations of $D(E)$ over the typical energy width Γ can be neglected [46, 47].

The main result of our previous work [24] was an equation for the thermalization dynamics of an observable O ,

$$\langle O(t) \rangle = (\langle O(t) \rangle_0 - \langle O(\infty) \rangle) e^{-2\Gamma t} + \langle O(\infty) \rangle, \quad (4)$$

with the additional equality $\langle O(\infty) \rangle = \overline{[O_{\alpha\alpha}]_{\alpha_0}}$, and

$$\overline{[O_{\alpha\alpha}]_{\alpha_0}} := \sum_\alpha \Lambda(\alpha_0, \alpha) O_{\alpha\alpha}, \quad (5)$$

is a microcanonical average of O around the initial state energy α_0 . $\overline{[O_{\alpha\alpha}]_{\alpha_0}}$ can be physically understood as an average over the set of free eigenstates that are involved in the time evolution of the system. $\langle O(t) \rangle_0$ represents the free dynamics under H_0 .

We now wish to study the time-averaged variance, or quantum fluctuations, of the local observable O , $\sigma_O^2(\infty) = \langle O^2(\infty) \rangle - \langle O(\infty) \rangle^2$, which can be obtained from Eq. (4) applied to O and O^2 ,

$$\sigma_O^2(\infty) = \overline{[\Delta O_{\alpha\alpha}^2]_{\alpha_0}}, \quad (6)$$

where $\overline{[\Delta O_{\alpha\alpha}^2]_{\alpha_0}} := \overline{[O_{\alpha\alpha}^2]_{\alpha_0}} - \overline{[O_{\alpha\alpha}]_{\alpha_0}}^2$. We recall a further result obtained in Ref. [24]: the time-fluctuations of O may be written as

$$\delta_O^2(\infty) = \frac{\overline{[\Delta O^2]_{\alpha_0}}}{4\pi D(E_{\alpha_0})\Gamma}. \quad (7)$$

From Eq. (6) and (7) we may already observe a remarkable feature of fluctuations of chaotic systems, that

is, their ratio after equilibration is given by,

$$\frac{\sigma_O^2(\infty)}{\delta_O^2(\infty)} = 4\pi D(E_{\alpha_0})\Gamma. \quad (8)$$

Eq. (8) is our first relevant result, and may be understood as a signature of quantum ergodicity in many-body systems, and further reveals the DOS in terms of only measurable quantities (see SM [47]).

Einstein Relation:— Now we show that Eq. (6) leads to the Einstein relation for the diffusion constant [48] in the limit $d_B \gg d_S \gg 1$, that is, a large system Hilbert space dimension. To observe this, we re-express $[\overline{O_{\alpha\alpha}}]_{\alpha_0}$ via,

$$[\overline{O_{\alpha\alpha}}]_{\alpha_0} = \sum_{s=-d_S/2}^{d_S/2} (O_S)_{ss} p(s), \quad (9)$$

where $p(s)$ may be written in terms of the DOS of the bath (see [47]),

$$p(s) = \frac{D_B(E_{\alpha_0} - \epsilon_s)}{\sum_{s=-d_S/2}^{d_S/2} D_B(E_{\alpha_0} - \epsilon_s)}. \quad (10)$$

To obtain the Einstein relation, we write $D_B(E) = D_0 \exp(\beta(E)E)$ where $\beta(E)$ is the inverse microcanonical temperature, which we assume changes slowly over the width Γ . To make a connection with classical Brownian motion we consider now $O_S = X$, with $X_{ss'} = s\delta_{s,s'}$ and $\epsilon_s = \frac{1}{2}ms^2$, interpreting the local quantum number s as the position in an harmonic oscillator potential. In the limit of small temperature relative to the system bandwidth, and large compared to the system energy spacing, $1 \ll m\beta \ll d_S$, we obtain,

$$\sigma_X^2(\infty) = [\overline{X_{\alpha\alpha}^2}]_{\alpha_0} = \frac{1}{m\beta(E_{\alpha_0})}. \quad (11)$$

Since $k_B T(E_{\alpha_0}) = \beta(E_{\alpha_0})^{-1}$ is the microcanonical temperature, we recover here the linear relation between the variance of the particle coordinate and the temperature that is found in Ornstein-Uhlenbeck (OU) processes (see [47]). Further, we note that Eq. (11) is an equipartition theorem, relating the average energy $\frac{1}{2}m\sigma_X^2(\infty)$ to the temperature. This occurs at the level of individual eigenstate averages $[\overline{X_{\alpha\alpha}^2}]_{\alpha_0}$, which motivates the description as an ‘eigenstate equipartition theorem’.

Quantum Jump Trajectories:— We turn now to the case in which we perform a set of subsequent quantum measurements, and assume that a non-degenerate local operator is measured. For the sake of clarity we consider again the operator X defined above, an initial state $|\psi(0)\rangle = |\epsilon_{s_0}\rangle|E_{\beta_0}^{(B)}\rangle$, and a set of N_m measurements separated by a time interval Δt , yielding a measurement record s_1, s_2, \dots, s_{N_m} . The sequence of ‘measurement quenches’ [49] is

$$|\epsilon_{s_0}\rangle|E_{\beta_0}^{(B)}\rangle \rightarrow |\epsilon_{s_1}\rangle|\psi_1^{(B)}\rangle \rightarrow |\epsilon_{s_2}\rangle|\psi_2^{(B)}\rangle \rightarrow \dots, \quad (12)$$

where $|\psi_j^{(B)}\rangle$ is the state of the bath at step j . Assuming that the total energy is not significantly perturbed by the measurement process, we can assume that the quantum dynamics is restricted to many-body states with energies close to the initial energy, $E_{\alpha_0} = \epsilon_{s_0} + E_{\beta}^{(B)}$. This assumption is valid assuming the range of system energies is negligible in comparison to the bath [47].

Eq. (4) is valid for any local observable and a different initial condition [24]. We define $p(s_f, s_i; t_f, t_i)$ as the probability of measuring the value s_f at time t_f , assuming that a previous observation yielded a value s_i at time t_i . Thus, we can apply Eq. (4) to the projector $P_{s_f} = |\epsilon_{s_f}\rangle_S \langle \epsilon_{s_f}| \otimes \mathbb{1}_B$, and obtain

$$p(s_f, s_i; t_f, t_i) = (\delta_{s_f, s_i} - p_{\infty}(s_f)) e^{-2\Gamma\Delta t} + p_{\infty}(s_f), \quad (13)$$

where $p_{\infty}(s_f) = [\overline{(P_{s_f})_{\alpha\alpha}}]_{\alpha_0}$, and $\Delta t = t_f - t_i$. $p_{\infty}(s_f)$ is the steady-state probability for the system to be in state s_f , which in the RMT approach can be written in terms of a microcanonical ensemble around the initial energy E_{α_0} .

Eq. (13) predicts that in the limit $\Delta t \gg 1/\Gamma$, the set of values s_1, \dots, s_{N_m} will be scattered with variance σ_X^2 . However, in the case $\Delta t < 1/\Gamma$, the measurement process will be able to temporally resolve the decay of the initial value of X . Actually, Eq. (13) predicts that the measurement outcomes form a Markov chain. Furthermore, we can show that the average over all the resulting stochastic trajectories of a measurement outcome, s_j at time t_j , is the same as the expectation value $\langle X(t_j) \rangle$ at time t_j [47]. In other words, if we measure the expectation value $\langle X(t_j) \rangle$, the value is independent of whether we have subjected the systems to a quantum measurement at times $t < t_j$ or not. Finally, deviations from Eq. (13) are expected for very short $\Delta t \ll t_Z$, with t_Z a typical quantum Zeno time-scale.

We may connect our discussion to the emergence of thermodynamic quantities through the non-equilibrium Gibbs entropy,

$$S_G(t) = - \sum_{s=-d_S/2}^{d_S/2} p(s, s_i; t, t_0) \ln p(s, s_i; t, t_0), \quad (14)$$

and its behaviour with Δt . In fact, from Eq. (4) we may show that $\frac{dS_G(t)}{dt} \geq 0$ [47]. The definition of a non-equilibrium Gibbs entropy for quantum jump trajectories makes an important connection to results in stochastic thermodynamics [50–52]. In particular, we have seen that $p(s, s_i; t, t_0)$ may be described by effective Langevin dynamics, and thus Eq. (14) may be seen to parallel the classical non-equilibrium Gibbs entropy defined in e.g. [50]. This construction further resembles the ‘observational entropy’ in Ref. [53].

We finally note that an entropy may be defined for an *individual* trajectory, by taking the probability distribution of measurement outcomes over all times. In

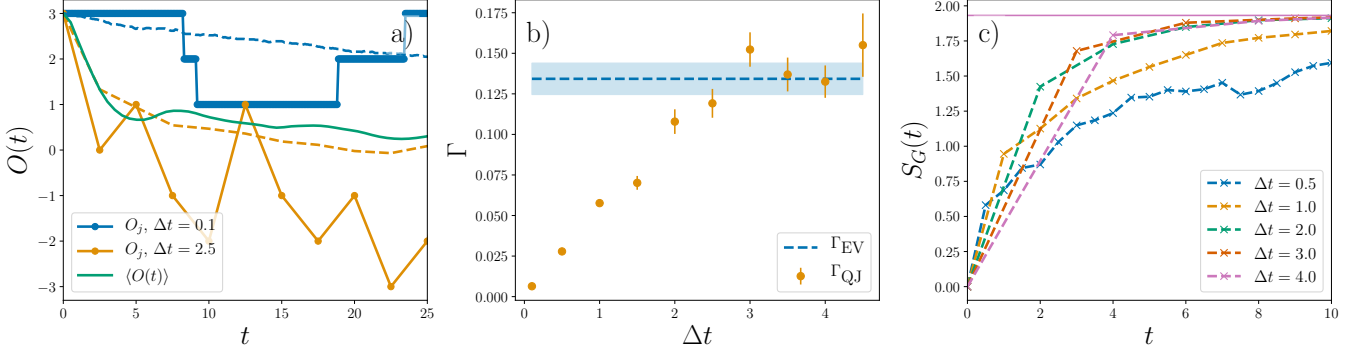


FIG. 2. Exact diagonalization calculations of Hamiltonian (15), (16). a) Examples of observable dynamics as obtained from $\langle O(t) \rangle$, quantum jump trajectories O_j , and their averages over 500 realizations (dashed lines). b) Convergence of the decay rate as measured by quantum jump trajectories (Γ_{QJ}) to that of thermalization dynamics (Γ_{EV}). Trajectories shown in SM [47]. c) Growth of the non-equilibrium Gibbs entropy. Solid line shows single trajectory entropy for $\Delta t = 4$ (see below Eq. (14)). Parameters: $J = 0.8, h_x = 0.7, S = 3, N = 4$.

equilibrium we have an equivalence between the quantum fluctuations $\sigma_O^2(\infty)$, and time-fluctuations of a single trajectory with $\Delta t \gg \Gamma^{-1}$, as each projective measurement occurs with a variance $\sigma_O^2(\infty)$. Thus, this entropy is equal to the maximal value of $S_G(t)$. This is confirmed numerically in Fig 2c).

Numerical calculations:— We have carried out numerical experiments to check the validity of the RMT model and its predictions with two basic sets of models:

- *Coupled quantum harmonic oscillators.* We consider a set of particles confined to move in a grid of discretized positions in one-dimensional harmonic potentials. The Hilbert space is formed by states $|s, i\rangle$, where $s = -S, \dots, S$ is the position in the i^{th} potential,

$$H_0 = \sum_{i=1}^N \sum_{s=-S}^S \epsilon_s |s, i\rangle \langle s, i| \quad (15)$$

with $\epsilon_s = s^2$. To this, we add the coupling term

$$V = h_x \sum_{i=1}^N \sum_{s=-S}^{S-1} (|s, i\rangle \langle s+1, i| + H.c.) + J \sum_{i=1}^{N-1} \sum_{s=-S}^{S-1} (|s, i\rangle \langle s+1, i+1| + |s+1, i\rangle \langle s, i+1| + H.c.), \quad (16)$$

which includes both a kinetic energy term proportional to h_x , and a hopping J between adjacent sites and energy levels in each oscillator. The observable is taken to be the oscillator position at $i = 1$, $O = X_1 = \sum_s s |s, 1\rangle \langle s, 1|$.

Numerical results are shown in Fig. 2. In particular, in Fig. 2b) we see that the decay rate of averaged quantum jump trajectories indeed converges to that of $\langle O(t) \rangle$ outside of the Zeno regime. Further, we observe in Fig. 2c) the growth of entropy in time to the value of the single trajectory entropy.

- *Quantum Spin-Chains.* The second system we consider is a Bilinear-Biquadratic spin-chain [54–56]. Details and

results are shown in the SM [47]. We note that the considered Hamiltonian does not have a quadratic energy dispersion, an assumption only required for the comparison to the OU process. Further, we consider both a local and global observable of this model, finding that our analysis is valid in each case - our assumptions simply require the observable has a sufficiently sparse structure in the free basis [24]. Finally, we note that the dynamics of this model shows multiple timescales, which are resolved by the dynamics of the quantum jump trajectories when Δt is of the relevant scale. This may allow quantum jump trajectories to resolve such phenomena as prethermalization [18].

In each case, we initialize the system a mid-energy eigenstate of the non-interacting Hamiltonian, H_0 , choosing such that $\langle O(0) \rangle = \max(O)$, and obtain Γ from a fit to Eq. (4).

Conclusions:— In this work we have shown how a closed quantum system initialized in a pure state may reproduce a *classical* temperature dependent fluctuation-dissipation theorem of Brownian motion. Specifically, we have reproduced the Einstein relation for the Ornstein-Uhlenbeck process. This result is a direct analytical observation of the emergence of classical statistical physics from unitary quantum dynamics. Indeed, we similarly observe an ‘eigenstate equipartition theorem’, and thus see that microcanonical temperature relations can be seen on the level of individual eigenstates, thus extending the intuition afforded by the ETH. Our results apply directly to quantum jump trajectories induced by repeated quantum measurements, finding that the variance of the trajectory is similarly described by a classical OU process.

Further, we have shown that the fluctuations of chaotic quantum systems may be exploited to accurately measure its density of states.

Our calculations are based on a random matrix the-

oretic approach, and build on earlier works where the current authors have obtained an analytic description of the full time-dependent decay to equilibrium [24]. The current work formalises an important consequence of this approach, the emergence of a description of the fluctuations of local observables in terms of a microcanonical temperature. This hints at a more fundamental foundation of classical statistical physics, as we see the important properties of this theory directly from the quantum dynamics of pure states. We have confirmed our results by a numerical exact diagonalization calculation on two model systems.

We acknowledge discussions with Edgar Roldán, and funding from project PGC2018-094792-B-I00 (MCIU/AEI/FEDER, UE), EPSRC grant no. EP/M508172/1, and from COST Action CA17113.

* C.Nation@sussex.ac.uk

† D.Porras@iff.csic.es

- [1] M. Schreiber, S. S. Hodgman, P. Bordia, H. P. Lüschen, M. H. Fischer, R. Vosk, E. Altman, U. Schneider, and I. Bloch, *Science* **349**, 842 (2015).
- [2] G. Clos, D. Porras, U. Warring, and T. Schaetz, *Phys. Rev. Lett.* **117**, 170401 (2016).
- [3] A. M. Kaufman, M. E. Tai, A. Lukin, M. Rispoli, R. Schittko, P. M. Preiss, and M. Greiner, *Science* **353**, 794 (2016).
- [4] C. Neill, P. Roushan, M. Fang, Y. Chen, M. Kolodrubetz, Z. Chen, A. Megrant, R. Barends, B. Campbell, B. Chiaro, A. Dunsworth, E. Jeffrey, J. Kelly, J. Mutus, P. J. O'Malley, C. Quintana, D. Sank, A. Vainsencher, J. Wenner, T. C. White, A. Polkovnikov, and J. M. Martinis, *Nat. Phys.* **12**, 1037 (2016).
- [5] C. Neill, P. Roushan, K. Kechedzhi, S. Boixo, S. V. Isakov, V. Smelyanskiy, A. Megrant, B. Chiaro, A. Dunsworth, K. Arya, R. Barends, B. Burkett, Y. Chen, Z. Chen, A. Fowler, B. Foxen, M. Giustina, R. Graff, E. Jeffrey, T. Huang, J. Kelly, P. Klimov, E. Lucero, J. Mutus, M. Neeley, C. Quintana, D. Sank, A. Vainsencher, J. Wenner, T. C. White, H. Neven, and J. M. Martinis, *Science* **360**, 195 (2018).
- [6] H. Kim, Y. Park, K. Kim, H. S. Sim, and J. Ahn, *Phys. Rev. Lett.* **120**, 180502 (2018).
- [7] J. Gemmer, A. Otte, and G. Mahler, *Phys. Rev. Lett.* **86**, 1927 (2001).
- [8] P. Reimann, *Phys. Rev. Lett.* **99**, 160404 (2007).
- [9] P. Reimann, *New Journal of Physics* **12**, 055027 (2010).
- [10] J. M. Deutsch, *New Journal of Physics* **12**, 075021 (2010).
- [11] A. J. Short, *New J. Phys.* **13**, 053009 (2011).
- [12] T. N. Ikeda, Y. Watanabe, and M. Ueda, *Phys. Rev. E* **84**, 021130 (2011).
- [13] T. Farrelly, F. G. S. L. Brandão, and M. Cramer, *Phys. Rev. Lett.* **118**, 140601 (2017).
- [14] F. Borgonovi, F. Mattiotti, and F. M. Izrailev, *Phys. Rev. E* **95**, 042135 (2017).
- [15] M. Rigol, V. Dunjko, and M. Olshanii, *Nature* **452**, 854 (2008).
- [16] L. D'Alessio, Y. Kafri, A. Polkovnikov, and M. Rigol, *Adv. Phys.* **65**, 239 (2016).
- [17] C. Gogolin and J. Eisert, *Rep. Prog. Phys.* **79**, 056001 (2016).
- [18] T. Mori, T. N. Ikeda, E. Kaminishi, and M. Ueda, *J. Phys. B. Atom. Molec. Phys.* **51**, 112001 (2018).
- [19] J. M. Deutsch, *Rep. Prog. Phys.* **81**, 082001 (2018).
- [20] L. P. García-Pintos, N. Linden, A. S. L. Malabarba, A. J. Short, and A. Winter, *Phys. Rev. X* **7**, 031027 (2017).
- [21] J. Richter, J. Gemmer, and R. Steinigeweg, *Phys. Rev. E* **99**, 050104 (2019).
- [22] M. Schiulaz, E. J. Torres-Herrera, and L. F. Santos, *Phys. Rev. B* **99**, 174313 (2019).
- [23] Á. M. Alhambra, J. Riddell, and L. P. García-Pintos, (2019), arXiv:1906.11280.
- [24] C. Nation and D. Porras, *Phys. Rev. E* **99**, 052139 (2019).
- [25] L. Dabelow and P. Reimann, (2019), arXiv:1903.11881.
- [26] F. Borgonovi, F. M. Izrailev, and L. F. Santos, *Phys. Rev. E* **99**, 010101 (2019).
- [27] D. Nickelsen and M. Kastner, *Phys. Rev. Lett.* **122**, 180602 (2019).
- [28] D. Nickelsen and M. Kastner, (2019), arXiv:1912.02043.
- [29] H. Hinrichsen, C. Gogolin, and P. Janotta, in *J. Phys.: Conference Series*, Vol. 297 (2011).
- [30] R. Ziener, A. Maritan, and H. Hinrichsen, *J. Stat. Mech.* **2015**, 8014 (2015).
- [31] G. Bisker, M. Polettini, T. R. Gingrich, and J. M. Horowitz, *J. Stat. Mech.*, 93210 (2017).
- [32] G. Manzano, R. Fazio, and E. Roldán, *Phys. Rev. Lett.* **122**, 220602 (2019).
- [33] M. V. Berry, *J. Phys. A: Math. Gen.* **10**, 2083 (1977).
- [34] M. Srednicki, *Phys. Rev. E* **50**, 888 (1994).
- [35] C. Nation and D. Porras, *New J. Phys.* **20**, 103003 (2018).
- [36] J. M. Deutsch, *Phys. Rev. A* **43**, 2046 (1991).
- [37] P. Reimann, *New J. Phys.* **17**, 055025 (2015).
- [38] G. Ithier and S. Ascroft, *J. Phys. A: Math. Th.* **51** (2018).
- [39] J. P. Garrahan and I. Lesanovsky, *Phys. Rev. Lett.* **104**, 160601 (2010).
- [40] L. F. Santos and M. Rigol, *Phys. Rev. E* **81**, 036206 (2010).
- [41] E. J. Torres-Herrera, J. Karp, M. Tavora, and L. F. Santos, *Entropy* **18** (2016).
- [42] F. Borgonovi, F. M. Izrailev, L. F. Santos, and V. G. Zelevinsky, *Physics Reports* **626**, 1 (2016).
- [43] P. Reimann, *Nat. Comms.* **7**, 10821 (2016).
- [44] J. M. Deutsch, (unpublished) (1991).
- [45] M. Srednicki, *J. Phys. A: Math. Gen.* **29**, L75 (1996).
- [46] C. Nation and D. Porras, *Quantum* **3**, 207 (2019).
- [47] See supplemental material.
- [48] R. Kubo, *Rep. Prog. Phys.* **29**, 255 (1966).
- [49] A. Bayat, B. Alkurtass, P. Sodano, H. Johannesson, and S. Bose, *Phys. Rev. Lett.* **121** (2018).
- [50] U. Seifert, *Phys. Rev. Lett.* **95**, 040602 (2005).
- [51] U. Seifert, *Rep. Prog. Phys.* **75**, 126001 (2012).
- [52] J. M. Parrondo, J. M. Horowitz, and T. Sagawa, *Nature Physics* **11**, 131 (2015).
- [53] D. Šafránek, J. M. Deutsch, and A. Aguirre, *Phys. Rev. A* **99**, 012103 (2019).
- [54] A. V. Chubukov, *Phys. Rev. B* **43**, 3337 (1991).
- [55] J. J. García-Ripoll, M. A. Martin-Delgado, and J. I. Cirac, *Phys. Rev. Lett.* **93** (2004).
- [56] A. Läuchli, G. Schmid, and S. Trebst, *Phys. Rev. B* **74** (2006).

Supplemental Material for Taking snapshots of a quantum thermalization process: emergent classicality in quantum jump trajectories

SUMMARY OF RMT FORMALISM

In this section we outline in brief the RMT methodology developed in Refs. [S1–S3], on which our calculations are based. We focus here on making clear the required assumptions on which the calculations rest, and refer the reader to the above references for details on the calculations themselves. Ref. [S1] provides a detailed formulation of the RMT model, and a derivation of the ETH, Ref. [S2] extends and formalises key features of observables, and describes time evolution of observables, and Ref. [S3] extends the approach to finite temperatures, and applies the method to an application on quantum computers and other devices. Self-averaging of chaotic wavefunctions is shown and discussed in the appendices of Ref. [S3]. Each of these works includes exact numerical calculations of realistic quantum spin-chains, which compare very well with the RMT framework.

Our summary below will be separated into two sections, the assumptions required on chaotic wavefunctions, and those on observables.

Assumptions on chaotic wavefunctions

The main assumption of our RMT formalism is the ansatz that the probability distribution on chaotic wavefunctions, $|\psi_\mu\rangle = \sum_\alpha c_\mu(\alpha)|\phi_\alpha\rangle$, is a Gaussian distribution with the constraint of mutual orthogonality, $\langle\psi_\mu|\psi_\nu\rangle = \delta_{\mu\nu}$,

$$p(c) = \frac{1}{Z} \exp \left(- \sum_{\mu\alpha} \frac{c_\mu^2(\alpha)}{2\Lambda(\mu, \alpha)} \right) \prod_{\substack{\mu\nu \\ \mu > \nu}} \delta \left(\sum_\alpha c_\mu(\alpha) c_\nu(\alpha) \right). \quad (\text{S1})$$

That is, the action of the interaction causes the eigenstate $|\psi_\mu\rangle$ to mix with sufficiently many approximately non-interacting states $|\phi_\alpha\rangle$ such that the distribution may be described by a Gaussian with some width $\Lambda(\mu, \alpha)$, with the requirement that the eigenstates remain orthogonal. The function Λ thus yields the envelope of the random wavefunctions. This function is shown to be a Lorentzian of width Γ for the particular RMT model which we use for comparison to our model, though it may be different for different models. In general for chaotic systems one may expect this function to be peaked around a certain energy, with a width $\Gamma(E)$ that may depend on the energy of the wavefunction. We show in [S3] that this change in width with energy can in fact be incorporated into our theory.

From Eq. (S1) one can calculate arbitrary correlation functions $\langle c_\mu(\alpha) \cdots c_\nu(\beta) \rangle_V$ of the model [S1]. We see that the largest correlation function that does not factorize is the four point correlation function,

$$\langle c_\mu(\alpha) c_\nu(\beta) c_{\mu'}(\alpha') c_{\nu'}(\beta') \rangle_V = \Lambda(\mu, \alpha) \Lambda(\nu, \beta) \delta_{\alpha\alpha'} \delta_{\beta\beta'} - \frac{\Lambda(\mu, \alpha) \Lambda(\nu, \beta) \Lambda(\mu, \alpha') \Lambda(\nu, \beta')}{\sum_\alpha \Lambda(\mu, \alpha) \Lambda(\nu, \alpha)} (\delta_{\alpha\beta} \delta_{\alpha'\beta'} + \delta_{\alpha\beta'} \delta_{\beta\alpha'}). \quad (\text{S2})$$

This can be understood in terms of Gaussian and non-Gaussian contractions, where the first term is that due to purely Gaussian behaviour (reminiscent of Wicks' theorem, for example), and the second term is due to the effective interactions between chaotic wavefunctions due to mutual orthogonality. We note that this term is actually crucial for a consistent description of observable matrix elements, and time-evolution. It is these correlation functions that form the basis for calculations in our framework.

Assumptions on observables

For the work outlined above there are two relevant assumptions to be made on the form of observables. The first, is that we assume that in the non-interacting basis the observable is diagonal, so $O_{\alpha\beta} \propto \delta_{\alpha\beta}$. We note that this is not a requirement for the general framework, which can be extended to observables that take instead a sparse structure in this basis [S2].

The second assumption can be summarized as ‘the ability to define a microcanonical average that does not vary pathologically in energy’. We will detail the specific requirements for this below, but note that this can be understood simply to be a minimal requirement on observables in order for thermalization to occur, as thermalization requires

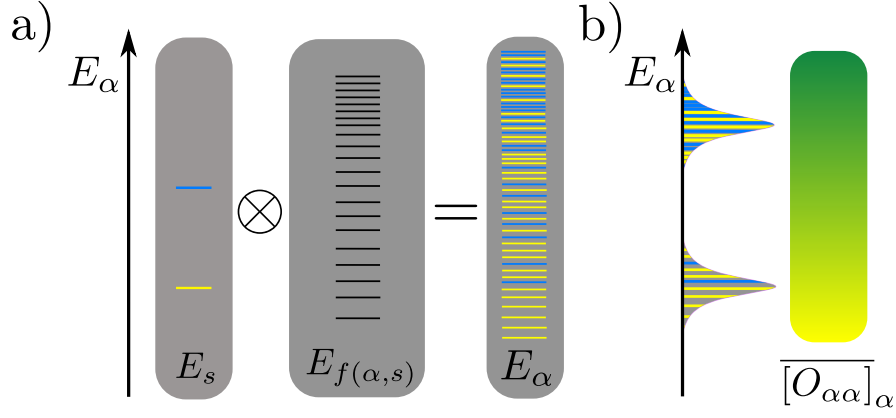


FIG. S1. a) Energy level diagram. Shown are two system energy levels E_s in distinct colors, the bath energy levels $E_{f(\alpha,s)}$, and the total system + bath energy levels E_α , coloured according to their respective system state. b) Illustration of microcanonical average $\overline{[O_{\alpha\alpha}]}_\alpha$. Each level in the average is weighted by the function Λ , this average is assumed to be made up of many energy levels, and to vary smoothly with energy.

that a system observables evolve to a microcanonical state that does not depend on the particular microstate of the initial state, rather on its energy alone.

In detail, then, this assumption requires that the microcanonical average

$$\overline{[O_{\alpha\alpha}]}_\mu := \sum_\alpha \Lambda(\mu, \alpha) O_{\alpha\alpha}, \quad (\text{S3})$$

is smooth over the width Γ of the function Λ . This is illustrated in Fig. S1. We showed in Ref. [S2] that this smoothness condition is fulfilled under the two conditions:

$$\begin{aligned} \frac{\Gamma}{\omega_0} &\gg 1 \\ \Gamma^2 \left| \frac{d^2 \overline{[O_{\alpha\alpha}]}_\mu}{dE_\mu^2} \right| &\ll 1. \end{aligned} \quad (\text{S4})$$

DERIVATION OF EQ. (9)

In this section we will evaluate

$$\overline{[O_{\alpha\alpha}]}_{\alpha_0} := \sum_\alpha \Lambda(\alpha_0, \alpha) O_{\alpha\alpha}. \quad (\text{S5})$$

The important point here is to realize that the Λ functions in the sum in Eq. (S5), which are Lorentzian distributions of width Γ , can be approximated as delta-functions (for small enough values of Γ); explicitly selecting those values such that $E_\alpha = E_{\alpha_0}$ in the summation,

$$\overline{[O_{\alpha\alpha}]}_{\alpha_0} = \sum_\alpha O_{\alpha\alpha} \frac{1}{D(E_{\alpha_0})} \frac{\Gamma_{\alpha_0}/\pi}{(E_\alpha - E_{\alpha_0})^2 + \Gamma_{\alpha_0}^2}. \quad (\text{S6})$$

Note that E_{α_0} and E_α can be interchanged in the definition of Λ , since we require that both Γ_α and $D(E_\alpha)$ vary negligibly over energy scales of the order of Γ_α . Under this very approximation we can change the Lorentzian by a Dirac delta function. Additionally, we work in the continuum limit, such that we may re-express the sum over α_B as

an integral over the bath eigenstates, $\sum_{\alpha_B} \rightarrow \int dE_{\alpha_B} D_B(E_{\alpha_B})$. We thus have,

$$\begin{aligned}
\overline{[O_{\alpha\alpha}]_{\alpha_0}} &= \sum_s O_{ss} \sum_{\alpha_B} \frac{1}{D(E_{\alpha_0})} \delta(E_{\alpha} - E_{\alpha_0}) \\
&= \sum_s O_{ss} \int dE_{\alpha_B} \frac{D_B(E_{\alpha_B})}{D(E_{\alpha_0})} \delta(E_{\alpha} - E_{\alpha_0}) \\
&= \sum_s O_{ss} \int dE_{\alpha_B} \frac{D_B(E_{\alpha_B})}{D(E_{\alpha_0})} \delta(\epsilon_s + E_{\alpha_B} - E_{\alpha_0}) \\
&= \sum_s O_{ss} D_B(E_{\alpha_0} - \epsilon_s) \frac{1}{D(E_{\alpha_0})} \\
&= \sum_s O_{ss} p(s).
\end{aligned} \tag{S7}$$

Here we have defined the probabilities

$$p(s) = \frac{D_B(E_{\alpha_0} - \epsilon_s)}{D(E_{\alpha_0})} = \frac{D_B(E_{\alpha_0} - \epsilon_s)}{\sum_s D_B(E_{\alpha_0} - \epsilon_s)}. \tag{S8}$$

Notably, for the special case where the bath density of states does not change over the entire system energy spectrum, we thus recover $p(s) = \frac{1}{d_S} \forall s$. This is a common assumption in formulations of statistical physics: that of *equal a-priori probabilities*. We thus observe the physical requirement for this common assumption of statistical physics to be valid within our theory.

DERIVATION OF EQ. (11)

In this section we show that

$$\begin{aligned}
\overline{[\Delta O_{\alpha\alpha}^2]_{\alpha_0}} &= \sum_s p(s) O_{ss}^2 - \left(\sum_s p(s) O_{ss} \right)^2 \\
&\sim \beta^{-1},
\end{aligned} \tag{S9}$$

for a system with a harmonic energy dispersion $E_s = \frac{1}{2} m s^2$.

In this case, we have the partition function

$$\mathcal{Z}(\beta) = \sum_s e^{-\beta E_s^2}, \tag{S10}$$

where s takes $2S + 1$ possible values from $[-S, S]$ (or more generally d_S values from $[-\frac{d_S}{2}, \frac{d_S}{2}]$), and $\beta = \beta(E_{\alpha})$. This can itself be evaluated as a Gaussian integral, $\sum_s \rightarrow \int_{-\infty}^{\infty} ds$, such that

$$\begin{aligned}
\mathcal{Z}(\beta') &= \int_{-\infty}^{\infty} ds e^{-\frac{1}{2} \beta' s^2} \\
&= \sqrt{\frac{2\pi}{\beta'}},
\end{aligned} \tag{S11}$$

where we have defined $\beta' := m\beta$. Now, the first term in Eq. (S9) can be written as

$$\begin{aligned}
\overline{[O_{\alpha\alpha}^2]_{\alpha_0}} &= \sum_s p(s) o_{ss}^2 \\
&= \frac{1}{\mathcal{Z}(\beta')} \sum_s s^2 e^{-\frac{1}{2} \beta' s^2} \\
&= \frac{1}{\mathcal{Z}(\beta')} \int_{-\infty}^{\infty} ds s^2 e^{-\frac{1}{2} \beta' s^2} \\
&= \frac{1}{\beta'}.
\end{aligned} \tag{S12}$$

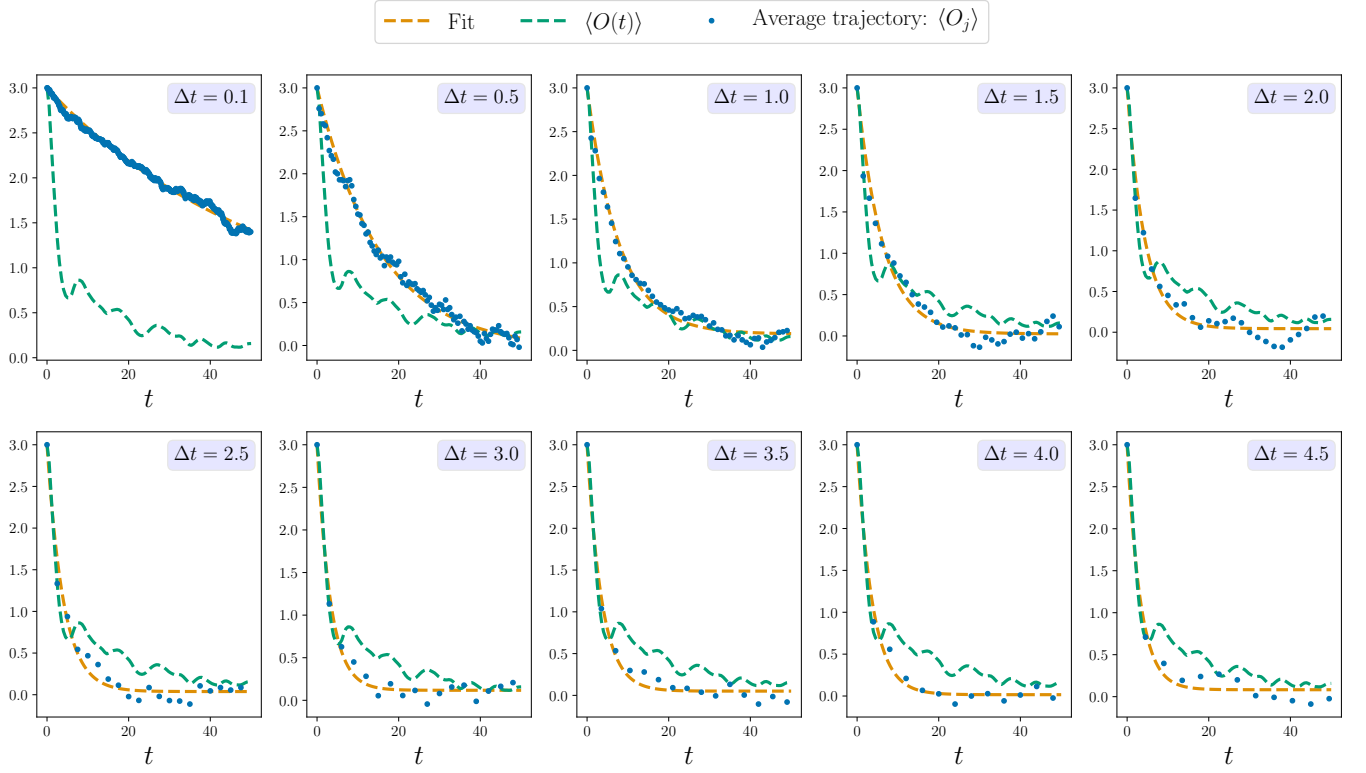


FIG. S2. Average quantum jump trajectories of $O = X_1$ quantum harmonic oscillator Hamiltonian of the main text for varying Δt . Here we see that as Δt is increased the decay rate of the average jump trajectory decays at the same rate as the expectation value (green dashed line). Orange dashed line shows fit to exponential decay used to obtain Γ_{QJ} in Fig. 2b). For small Δt , the decay is slowed due to proximity to the Zeno regime of completely frozen dynamics at $\Delta t \rightarrow 0$. Averages over 500 realizations of quantum trajectories (100 realizations for $\Delta t = 0.1, 0.5$). Parameters: $J = 0.8, h_x = 0.7, S = 3, N = 4$.

Now, the second term in Eq. (S9), can be seen along the same lines to be trivially zero, we thus have,

$$\overline{[O^2_{\alpha\alpha}]_{\alpha_0}} = \frac{1}{m\beta}. \quad (\text{S13})$$

QUANTUM JUMP TRAJECTORIES

Thermalization of Quantum Jump Trajectories

We can show that, according to expression (13), the probability distribution of measurement outcomes at a given time t is independent of measurements having been performed at times between 0 and t . This implies that the average over quantum jump trajectories of the measurement outcome of an observable, O , at some time t , is the same as the expectation value $\langle O(t) \rangle$ in the absence of previous quantum measurements.

This can be shown with the following relation. Assume that a measurement yields a value s_i at time t_i and a future observation yields the value s_f at time t_f . At some intermediate time, an observation is performed a time $t_i < t' < t_f$,

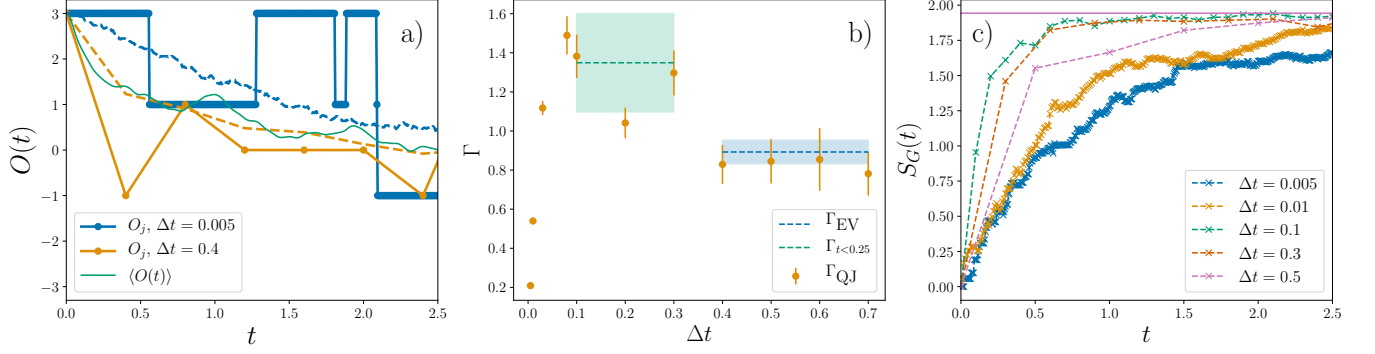


FIG. S3. Exact diagonalization calculations of spin-chain Hamiltonian of Eq. (S20) for $O = S_z^1$. a) Examples of observable dynamics as obtained from $\langle O(t) \rangle$, quantum jump trajectories O_j , and their averages over 100 realizations (dashed lines). b) Convergence of the decay rate as measured by quantum jump trajectories to that of thermalization dynamics. Trajectories shown in SM [S47]. c) Growth of the non-equilibrium Gibbs entropy. Solid line shows single trajectory entropy for $\Delta t = 0.5$. Parameters: $N = 4, S = 3, h_z = 1, h_x = 0.2, J = 0.8, \Delta = 0.3, q = 1.5$.

with outcome s' . From simple algebra it follows that the conditioned probability distribution in (13) satisfies that,

$$\begin{aligned}
 \sum_{s_m} p(s_f, s_m; t_f, t_m) p(s_m, s_i; t_m, t_i) \\
 &= \sum_{s_m} \left((\delta_{s_f, s_m} - p_\infty(s_f)) e^{-2\Gamma(t_f - t_m)} + p_\infty(s_f) \right) \left((\delta_{s_m, s_i} - p_\infty(s_m)) e^{-2\Gamma(t_m - t_i)} + p_\infty(s_m) \right) \quad (S14) \\
 &= (\delta_{s_f, s_i} - p_\infty(s_f)) e^{-2\Gamma(t_f - t_i)} + p_\infty(s_f) \\
 &= p(s_f, s_i; t_f, t_i).
 \end{aligned}$$

By induction Eq. (S14) can be extended to the case where an average is taken over a set of intermediate measurement outcomes, yielding the result that the average distribution probability at some time is independent of whether the system was monitored or not. This result is of course not valid in the Zeno regime, where the exponential decay assumption is not valid.

We show examples of the decay of average quantum jump trajectories in Fig. S2. These are the same trajectories used to obtain the decay rates in Fig. 2b).

Derivation of the 2nd law

In this section we will bound the derivative of the non-equilibrium Gibbs entropy. To simplify notation, we write $p(s_f, s_i; t_f, t_0) = p(s_f; t)$, such that

$$S_G(t) = - \sum_{s=-d_S/2}^{d_S/2} p(s, t) \ln p(s, t), \quad (S15)$$

for

$$p(s, t) = p(s, 0) e^{-2\Gamma t} + (1 - e^{-2\Gamma t}) p_\infty(s), \quad (S16)$$

where $p_\infty(s)$ is the equilibrium probability of obtaining the outcome s from a measurement of O . We have, then, that

$$\frac{dS_G(t)}{dt} = - \sum_s [2\Gamma e^{-2\Gamma t} (p_\infty(s) - p(s, 0)) (\ln p(s, t) + 1)] \quad (S17)$$

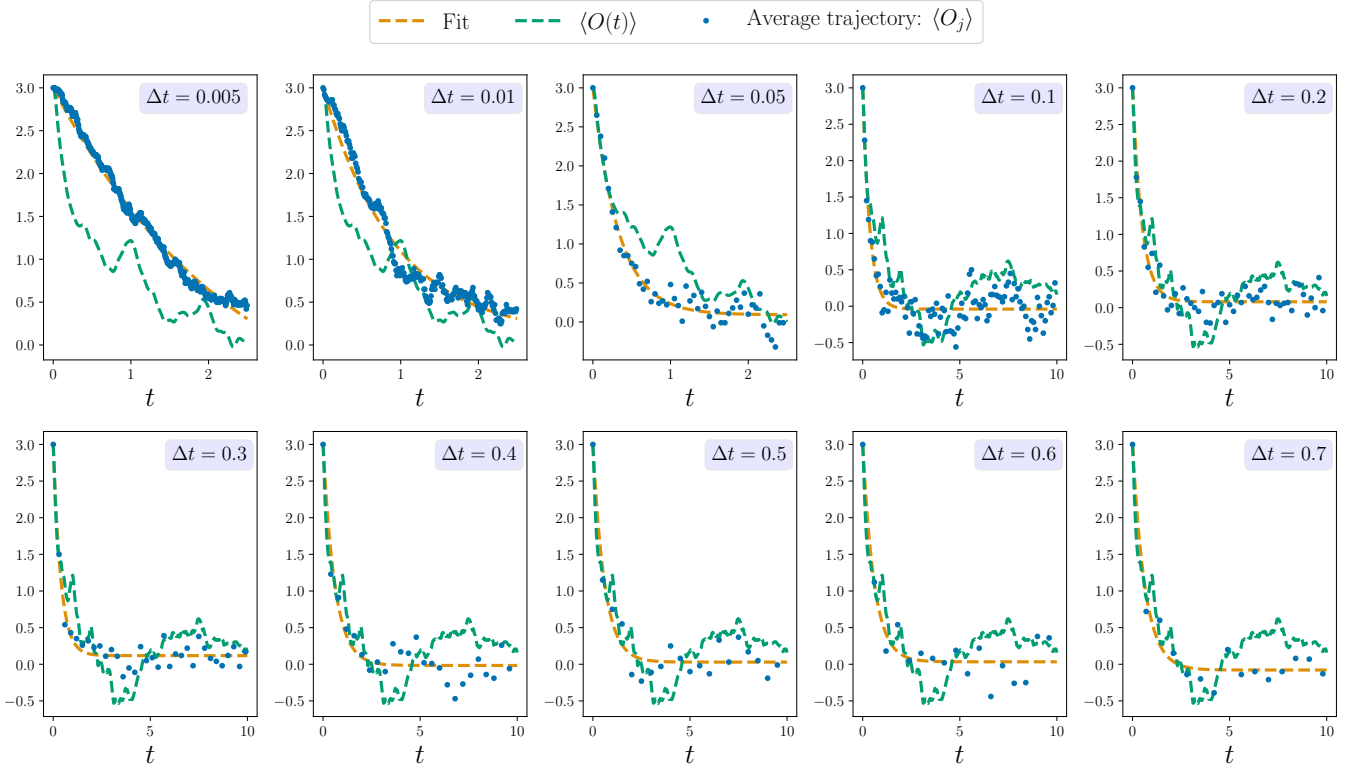


FIG. S4. Average quantum jump trajectories of $O = S_z^1$ of spin-chain Hamiltonian of Eq. (S20) for varying Δt . Here we see that as Δt is increased the decay rate of the average jump trajectory decays at the same rate as the expectation value (green dashed line). Orange dashed line shows fit to exponential decay used to obtain Γ_{QJ} in Fig. S3b). For small Δt , the decay is slowed due to proximity to the Zeno regime of completely frozen dynamics at $\Delta t \rightarrow 0$. Averages over 100 realizations of quantum trajectories. Parameters: $N = 4, S = 3, h_z = 1, h_x = 0.2, J = 0.8, \Delta = 0.3, q = 1.5$.

which, using that $1 - \frac{1}{x} \leq \ln x \leq x - 1$, we obtain

$$\begin{aligned} \frac{dS_G(t)}{dt} &\geq 2\Gamma e^{-2\Gamma t} \left[\sum_s (p(s, 0)p(s, t) - p_\infty(s)(2 - \frac{1}{p(s, t)})) \right] \\ &\geq 2\Gamma e^{-2\Gamma t} [p(s_0, t) - 2 + \sum_s \frac{1}{p(s, t)}] \end{aligned} \quad (\text{S18})$$

where in the second line we have used that $p(s, 0) = \delta_{s, s_0}$, where s_0 is the initial value of O_S . Now, we can thus see that at $t \rightarrow 0$, the factor $\sum_s \frac{1}{p(s, t)} \rightarrow \infty$. This indicates that at early times the entropy grows faster for smaller Δt , as observed in Fig. 2c) of the main text. For $t > 0$, we can note that $\frac{1}{p(s, t)} \geq 1$ and $p(s_0, t) \geq 0$, so

$$\frac{dS_G(t)}{dt} \geq 2\Gamma e^{-2\Gamma t} [d_s - 2] > 0, \quad (\text{S19})$$

for observables with more than one possible outcome $d_s \geq 2$.

Interpreting this result, we note that $S_G(t)$ is defined for quantum jump trajectories only at times $j\Delta t$, and we have that $p(s, t)$ follows the RMT result between successive measurements. We thus see that, averaged over trajectories, the Gibbs entropy can be seen to increase between successive measurements.

ADDITIONAL NUMERICAL RESULTS

In this section we present some complementary numerical results to the results of the main text. Firstly, we present in Fig. S2 the corresponding quantum jump trajectories to the decay rate plot of Fig. 2b) of the main text. These

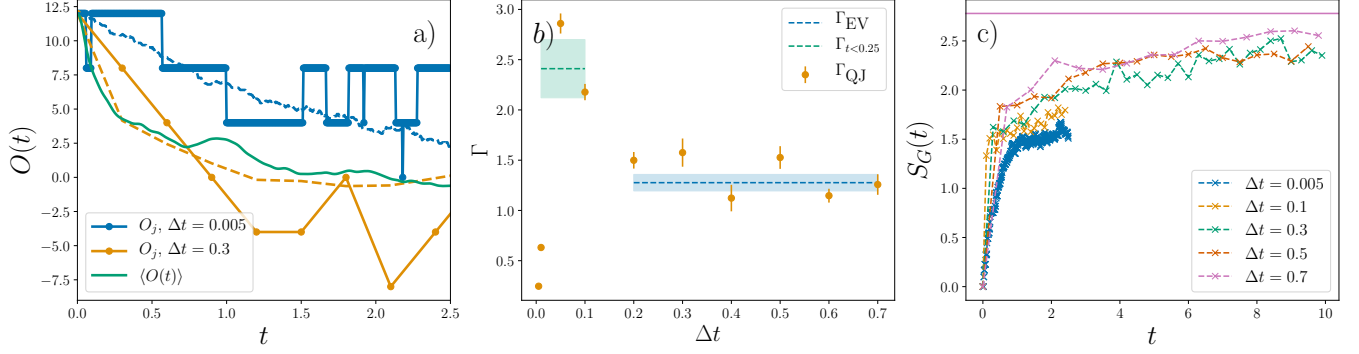


FIG. S5. Exact diagonalization calculations spin-chain Hamiltonian of Eq. (S20) for global observable $O = \sum_i^N S_z^i$. a) Examples of observable dynamics as obtained from $\langle O(t) \rangle$, quantum jump trajectories O_j , and their averages over 100 realizations, indicated by $\langle O_j \rangle$ (dotted lines). b) Convergence of the decay rate as measured by quantum jump trajectories to that of thermalization dynamics. Trajectories shown in SM [S47]. c) Growth of the non-equilibrium Gibbs entropy. Solid line shows single trajectory entropy for $\Delta t = 0.7$. Parameters: $N = 4, S = 3, h_z = 1, h_x = 0.2, J = 0.8, \Delta = 0.3, q = 1.5$.

show the decay of the expectation value, as well as the quantum jump trajectories for different values of Δt , to which we perform a fit. Notice that for Δt outside of the Zeno regime, we observe the quantum jump trajectories thermalize at approximately the same rate as the expectation value.

Quantum Spin Chain Results

In Fig. S3 we show complementary results to Fig. 2 of the main text for the large S spin-chain given by the Hamiltonian

$$H_0 = \sum_j^N \left[h_z S_z^j + h_x S_x^j \right], \quad (\text{S20})$$

where $j = 1$ is the system spin. The coupling Hamiltonian is

$$V = \frac{1}{2} J \sum_i^{N-1} \left[S_x^i S_x^{i+1} + S_y^i S_y^{i+1} + \Delta S_z^i S_z^{i+1} + q \left((S_x^i S_x^{i+1})^2 + (S_y^i S_y^{i+1})^2 + \Delta (S_z^i S_z^{i+1})^2 \right) + H.c \right], \quad (\text{S21})$$

where $S_{x,y,z}^i$ are spin operators on site i . Notice that this Hamiltonian does not have a quadratic energy dispersion of the system at $i = 1$ - this is required only to obtain the Einstein relation in the form of the OU process.

The contributing thermalization dynamics of both the expectation values and quantum jump trajectories, used to obtain Fig. S3b), are shown in Fig. S4. Here we have used the observable $O = S_z^1$.

Interestingly, we observe that the expectation value dynamics consist of two separate timescales. At very short times, the decay is fast, however after some time, a slower decay dominates. Notice that this more complicated dynamics is mirrored in the quantum jump trajectories. In Fig. S3b), unlike the harmonic oscillator chain, the quantum jump trajectory decay rate is actually faster than the expectation value decay for a range of Δt . For this intermediate range of Δt values, the quantum jump trajectories decay at the same rate as the short time dynamics of the expectation value. As Δt is increased, the decay rate slows to that of a fit to the whole dynamics of the trajectory.

We thus see that more complex dynamics may also be resolved in the quantum jumps framework. Indeed, the approach from quantum chaos, employing Eq. (S1), is more general than the specific RMT model applied in the main text, and may describe systems where Λ is of a different form to a Lorentzian. In such cases, the decay deviates from a purely exponential form.

Global Observables

The theory developed in the main text does not require that the observable is strictly local, rather that is diagonal in the basis of eigenstates of the non-interacting Hamiltonian. In-fact, even this requirement is not necessary in our

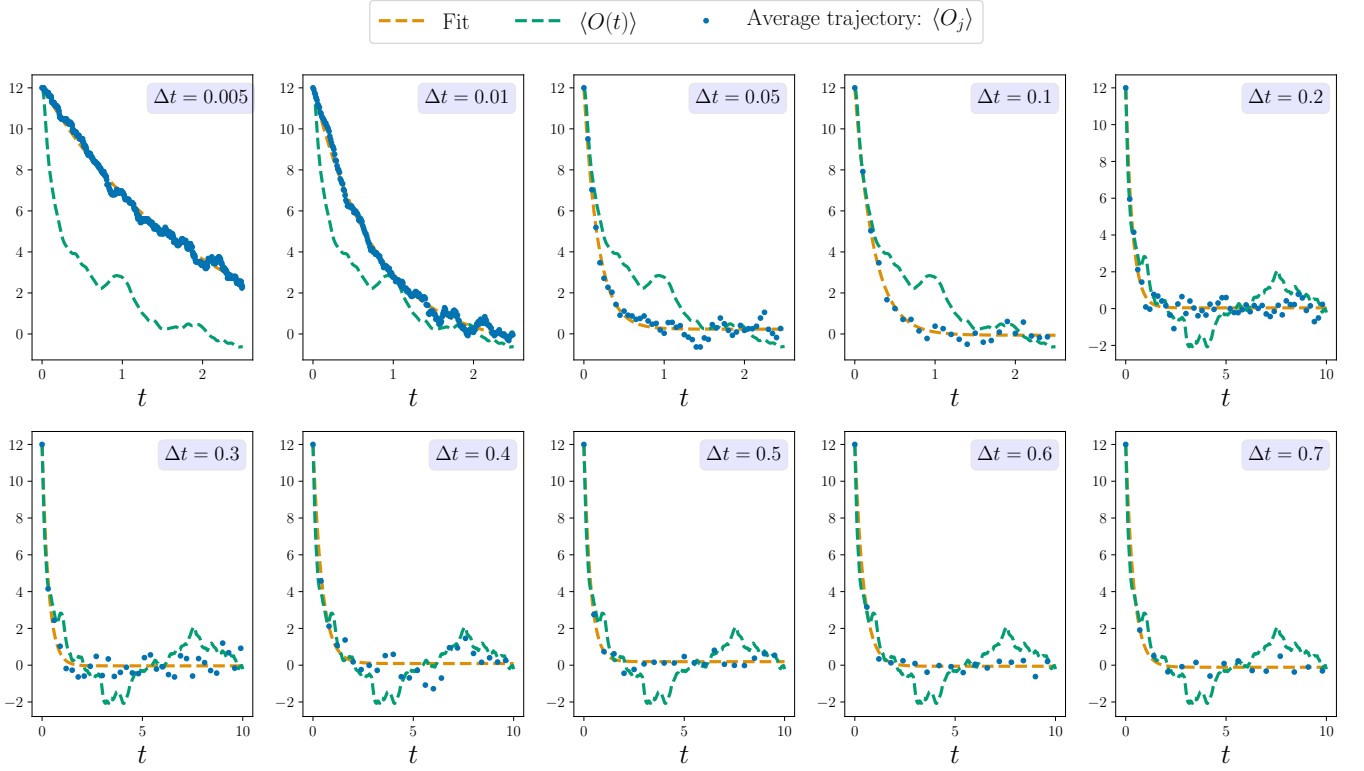


FIG. S6. Average quantum jump trajectories of $O = \sum_i S_z^i$ of spin-chain Hamiltonian of Eq. (S20) for varying Δt . Here we see that as Δt is increased the decay rate of the average jump trajectory decays at the same rate as the expectation value (green dashed line). Orange dashed line shows fit to exponential decay used to obtain Γ_{QJ} in Fig. S5b). For small Δt , the decay is slowed due to proximity to the Zeno regime of completely frozen dynamics at $\Delta t \rightarrow 0$. Averages over 100 realizations of quantum trajectories. Parameters: $N = 4, S = 3, h_z = 1, h_x = 0.2, J = 0.8, \Delta = 0.3, q = 1.5$.

RMT framework, rather the observable must be sufficiently sparse, and may be formulated in terms of sums of local observables $O = \sum_i O_i$ that are not necessarily diagonal [S2].

We can thus apply this approach to global observables of the system. Here we use the spin-chain system of Eq. (S20), and choose as our observable $O = \sum_j S_z^j$. We see in Figs. S5 and S6 that our analysis of the main text still holds in this case.

Total Energy

Here we give some additional numerical results in order to verify the results of the main text. First, we note that an assumption made above is that the energy does not change in time significantly due to the action of measurements in a quantum jump trajectory. This is a reasonable assumption in the limit of a very large bath, where the system contributes little to the total energy. We confirm this assumption for the numerical models studied, where the bath is of a modest size, in Fig. S7.

Measurement of the Density of States

In the main text we obtained the fluctuation relation

$$\frac{\sigma_O^2(\infty)}{\delta_O^2(\infty)} = 4\pi D(E)\Gamma, \quad (\text{S22})$$

which we show in this section via numerical exact diagonalizations may be exploited to measure the density of states of a quantum system. We show this for two models, the first is the quantum harmonic oscillator model of the main

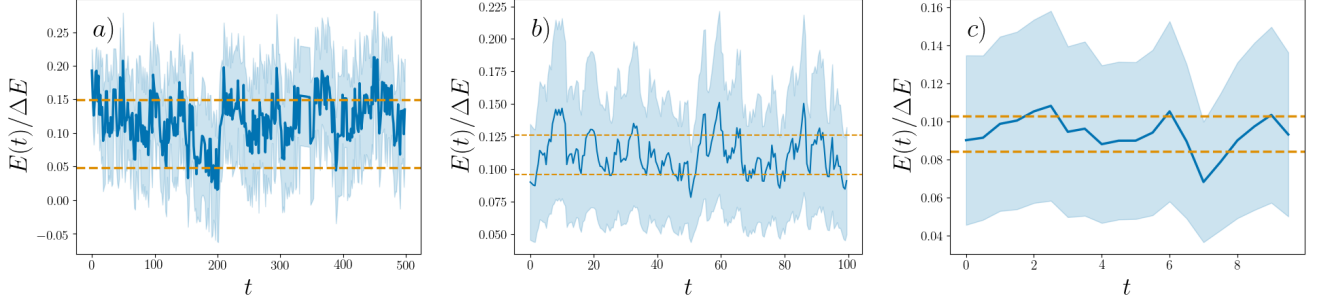


FIG. S7. Change of total energy $E(t) = \langle H(t) \rangle$ in time due to action of repeated projective measurements (blue solid line). Variance of energy $\sigma_E(t)$ shown in shaded area. Dashed lines show time-fluctuations of energy $\delta_E(\infty)$. $\Delta E = E_{max} - E_{min}$. a) Quantum harmonic oscillator chain of main text, Parameters: $J = 0.8, h_x = 0.7, S = 3, N = 4$. Time averages variance $\overline{\sigma_E(t)}$ of order $\frac{\sigma_E(t)}{\Delta E} \approx 0.05$ b) and c) Spin chain of Eq. (S20) under action of local observable S_z^1 and global observable $\sum_i S_z^i$ respectively. $\frac{\sigma_E(t)}{\Delta E} \approx 0.015, 0.009$ for local and global observables respectively. Parameters: $N = 4, S = 3, h_z = 1, h_x = 0.2, J = 0.8, \Delta = 0.3, q = 1.5$

text. The second model we use is a chain of spin- $\frac{1}{2}$ particles, which more closely resembles an ion chain or other system of qubits. Eq. S22 applies to such models, as this relation does not require any assumptions on the system observable other than the requirement that it is diagonal in the non-interacting eigenbasis, and thus a large system dimension is not required.

The spin- $\frac{1}{2}$ chain is described by a Hamiltonian of the form,

$$H = H_S + H_B + H_{SB}, \quad (\text{S23})$$

where H_S describes a single spin in a B_z field

$$H_S = B_z^{(S)} \sigma_z^{(1)}. \quad (\text{S24})$$

Here $\{\sigma_i^{(j)}\}$ $i = x, y, z$ are the Pauli operators acting on site j . We take the system as site $j = 1$. The bath Hamiltonian is a spin-chain of length $N - 1$, with nearest-neighbour Ising and XX interactions subjected to both B_z and B_x fields

$$H_B = \sum_{j>1}^N (B_z^{(B)} \sigma_z^{(j)} + B_x^{(B)} \sigma_x^{(j)}) + \sum_{j>1}^{N-1} (J_z \sigma_z^{(j)} \sigma_z^{(j+1)} + J_x (\sigma_+^{(j)} \sigma_-^{(j+1)} + \sigma_-^{(j)} \sigma_+^{(j+1)})). \quad (\text{S25})$$

The interaction Hamiltonian describes the coupling of the system spin to a single central bath ion of index $N_m = 3$,

$$H_{SB} = J_z^{(SB)} \sigma_z^{(1)} \sigma_z^{(N_m)} + J_x^{(SB)} (\sigma_+^{(1)} \sigma_-^{(N_m)} + \sigma_-^{(1)} \sigma_+^{(N_m)}). \quad (\text{S26})$$

For the initial state of the spin- $\frac{1}{2}$ system we choose a randomly selected eigenstate of $H_0 = H_S + H_B$, ensuring only that the initial system state is $|\uparrow\rangle$, and that the initial energy is in the central $\frac{1}{2}$ of the total energy spectrum (guaranteeing that it is not too close to the ground state).

Numerics confirming Eq. (S22) are shown for both the quantum harmonic oscillator of the main text and the above spin- $\frac{1}{2}$ chain in Figs. S8 a) and b) respectively.

In the exact diagonalization calculations in Fig. S8 we have calculated $D(E)$ in two ways. The first is the exact value obtained numerically, and the second is a numerical experiment performed by calculating the σ_O^2 and δ_O^2 and Γ from the expectation value dynamics $\langle O(t) \rangle$ of a local observable (σ_z for the chain of spin- $\frac{1}{2}$ particles, the same as in the main text for the remaining models). Each of these three quantities are obtainable in a realistic experimental scenario, and thus this approach may be exploited in order to measure the DOS of a many-body quantum system.

ORNSTEIN-UHLENBECK PROCESS

In the main text we make comparisons of the results to the classical dynamics of the Ornstein-Uhlenbeck (OU) process, describing the Brownian motion [S4] of the position $x(t)$ of a particle in a medium subjected to random

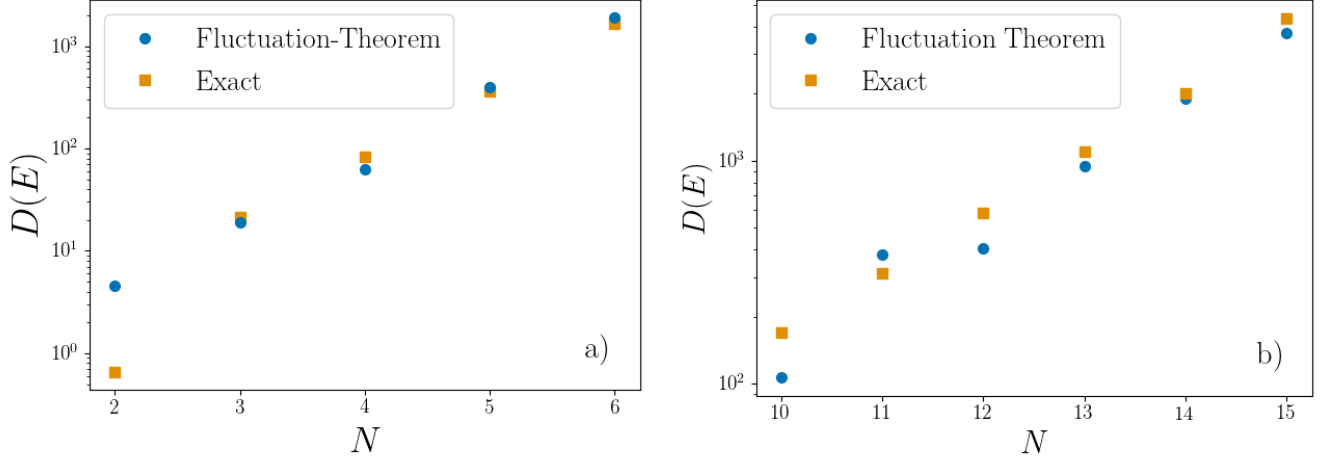


FIG. S8. Comparison of density of states as inferred from the fluctuation theorem of Eq. (S22) (yellow squares) with exact value (blue circles). a) For system of coupled quantum harmonic oscillators described in main text. Parameters: $J = 1.2$, $h_x = 0.8$, $S = 2$ b) For chain of spin- $\frac{1}{2}$ particles with Hamiltonian (S23). Parameters: $B_x^{(S)} = 0$, $B_z^{(B)} = 0$, $B_x^{(B)} = 0.3$, $J_x^{(S)} = 0.4$, $J_z^{(S)} = 0.2$, $J_z^{(B)} = 0.1$, $J_x^{(B)} = 1$, $B_z^{(S)} = 0.8$.

collisions with its environment. We summarize the relevant results here, and show a modification that reproduces the same finite-size time-fluctuations as the RMT model of the main text.

The OU process is described by the Langevin equation,

$$\frac{dx(t)}{dt} = -\frac{k}{\gamma}(x(t) - \bar{x}) + \xi(t), \quad (\text{S27})$$

where γ and \bar{x} are constants, and $\xi(t)$ is a stochastic random variable fulfilling $\langle \xi(t) \rangle_\xi = 0$, $\langle \xi(t)\xi(t') \rangle_\xi = 2D\delta(t - t')$, where $\langle \cdots \rangle_\xi$ indicates an average over stochastic trajectories, and D is the diffusion constant. The OU process describes the motion of an overdamped harmonic oscillator driven by white noise, with an oscillator potential $V(x) = \frac{k}{2}x^2$. This is easily solved [S5, S6] to find (setting $\bar{x} = 0$) $x(t) = x(0)e^{-\frac{k}{\gamma}t}$ and $\langle x^2(t) \rangle_\xi = \langle x(t) \rangle_\xi^2 + \frac{D\gamma}{k}(1 - e^{-2\frac{k}{\gamma}t})$. The long-time observable variance may be written as $\sigma_x^2(\infty) = \frac{D\gamma}{k}$. For a system in thermal equilibrium, the time-average energy is $\langle E \rangle = \frac{1}{2}k_B T$ by the equipartition theorem. We then see that the long-time average energy gives $\langle V \rangle = \frac{1}{2}D\gamma$, such that $D = \frac{k_B T}{\gamma}$. This is the celebrated Einstein relation of Brownian motion, a manifestation of the fluctuation-dissipation theorem (FDT) [S7]. Note that in the case of the OU process the equipartition theorem is invoked in order to obtain the Einstein relation, whereas for our description in terms of chaotic wavefunctions both can be observed to emerge simultaneously, and are encompassed in Eq. (11) of the main text.

We further note that if one modifies the stochastic noise $\xi(t)$ such that $\langle \xi(t) \rangle_\xi = v(s)$, with v a random variable itself, with $\overline{v(s)} = 0$, and $\overline{v(s)v(s')} = v^2\delta(s - s')$, we obtain,

$$\delta_x^2(\infty) = \frac{v^2\gamma^2}{k^2}. \quad (\text{S28})$$

Note that the physical interpretation of this modification is a shaking of the harmonic trap with white noise at a random velocity v for any given realization of the random force ξ . In this case, we can make the association

$$v^2 \Rightarrow \frac{[\overline{\Delta O^2}]_{\alpha_0} \Gamma}{4\pi D(E)} = \frac{k_B T \Gamma}{4\pi D(E) m}. \quad (\text{S29})$$

The modified time-fluctuation can be thought of as an equivalent of the Einstein relation for time-fluctuations of finite classical systems.

* C.Nation@sussex.ac.uk

[†] D.Porras@iff.csic.es

- [S1] C. Nation and D. Porras, New J. Phys. **20**, 103003 (2018).
 - [S2] C. Nation and D. Porras, Phys. Rev. E **99**, 052139 (2019).
 - [S3] C. Nation and D. Porras, Quantum **3**, 207 (2019).
 - [S4] A. Einstein, Ann. Phys. **17**, 549 (1905).
 - [S5] J. L. Doob, The Annals of Mathematics **43**, 351 (1942).
 - [S6] G. E. Uhlenbeck and L. S. Ornstein, Phys. Rev. **36**, 823 (1930).
 - [S7] R. Kubo, Rep. Prog. Phys. **29**, 255 (1966).
-